J|A|C|S
ARTICLES
Published on Web 06/14/2002

Binding Efficiency and Transport Properties of Molecularly Imprinted Polymer Thin Films

Daniel J. Duffy,† Kanad Das,† Shaw L. Hsu,*,‡ Jacques Penelle,*,‡ Vincent M. Rotello,*,† and Howard D. Stidham†

Contribution from the Department of Chemistry and the Department of Polymer Science and Engineering, University of Massachusetts, Amherst, Massachusetts 01003

Received January 23, 2002

Abstract: A model system for the characterization of molecular recognition events in molecularly imprinted polymers (MIPs) is presented. The use of a biologically inspired, three-point hydrogen-bonding motif and a thin film polymeric matrix allows for pre- and post-polymerization binding properties to be characterized by infrared spectroscopy. A method to determine binding constants was developed and utilized before and after cross-linking. These values showed a 10-fold decrease in binding after polymerization, which was attributed to an increase in molecular confinement after polymerization and a change in the local structural environment of the binding cavity. Transport of the guest molecule was shown to be reversible.

Introduction

Molecular imprinting is a powerful way to achieve three-dimensional molecular recognition via the template-directed synthesis of highly cross-linked polymeric matrices.[1−3] Imprinted polymers are useful materials for molecular recognition due to the specificity that arises from complementary interfaces between the guest molecules and the polymeric host environment based on the general principles of supramolecular chemistry. They have been used as sensors,[4−6] chromatographic columns,[7,8] and mimics for biological receptors,[9−11] enzymes,[9−15] and antibodies.[16]

A common approach to the synthesis of imprinted polymers involves the association of host−guest molecules added to the monomers prior to polymerization. Free-radical polymerizations are typically used due to their functional group tolerance. After polymerization (cross-linking) and guest removal, the resulting polymer can be demonstrated by a variety of techniques to maintain structural "memory" of the electronic and geometric nature of the guest molecule used as the template. Imprinting involves the additive effect of a large number of complex processes that take place at various length scales.[17] The host−guest chemistry is affected by the local molecular environment while the dynamics and mobility of the template molecules is related to the cross-linking of the polymeric matrix. Usually the samples do not provide an efficient mechanism for local temperature control during exothermic polymerization reactions, and this leads to nonequilibrium structures. The result is a final polymer morphology that is heterogeneous at length scales only slightly larger than the size of the imprinted cavities. This heterogeneous character affects the optimal release and uptake of specific target molecules, and certainly influences the post-polymerization binding.

To provide a generalized model for the imprinting process that can address the local and general features of the imprinted polymeric matrices, an experimental, multidisciplinary methodology was designed to address the inherent complexity of a well-controlled imprinting system.[18] Our design is based on the use of a biologically inspired, well-defined, three-point hydrogen-bonding motif formed by the complex between thymine and 2,6-diacyl diaminopyridine moieties shown in Figure 1. This motif provides a robust recognition unit with binding characteristics that can readily be characterized. The binding characteristics of this system are well-known in solution.[19−21] In addition, this motif offers a very convenient molecular tag to

* To whom all correspondence should be addressed. E-mail: slhsu@polysci.umass.edu.
† Department of Chemistry.
‡ Department of Polymer Science and Engineering.

(1) Whitcombe, M. J.; Vulfson, E. *Adv. Mater.* **2001**, *13*, 467.
(2) Shea, K. J.; Stoddard, G. J.; Shavelle, D. M.; Wakul, F.; Choate, R. M. *Macromolecules* **1990**, *23*, 4497.
(3) Steinke, J.; Sherrington, D. C.; Dunkin, I. R. *Adv. Polym. Sci.* **1995**, *123*, 81.
(4) Lubke, C.; Lubke, M.; Whitcombe, M. J.; Vulfson, E. N. *Macromolecules* **2000**, *33*, 5098.
(5) Liang, C.; Peng, H.; Zhou, A.; Nie, L.; Yao, S. *Anal. Chim. Acta* **2000**, *415*, 135.
(6) Matsui, J.; Fujiwara, K.; Ugata, S.; Takeuchi, T. *J. Chromatogr. A* **2000**, *899*, 25.
(7) Wulff, G.; Vesper, W. *J. Chromatogr.* **1978**, *167*, 171.
(8) Yoshikawa, M.; Fujisawa, T.; Izumi, J. *Macromol. Chem. Phys.* **1999**, *200*, 1458.
(9) Piletsky, S. A.; Panasyuk, T. L.; Piletskaya, E. V.; Nicholls, I. A.; Ulbricht, M. *J. Membr. Sci.* **1999**, *157*, 263.
(10) Piletsky, S. A.; Matuschewski, H.; Schedler, U.; Wilpert, A.; Pieletska, E. V.; Thiele, T. A.; Ulbricht, M. *Macromolecules* **2000**, *33*, 3092.
(11) Fischer, L.; Muller, R.; Ekberg, B.; Mosbach, K. *J. Am. Chem. Soc.* **1991**, *113*, 9358.
(12) Wulff, G.; Grobe-Einsler, R.; Vesper, W.; Sarhan, A. *Makromol. Chem.* **1977**, *178*, 2817.
(13) Wulff, G.; Vesper, W.; Grobe-Einsler, R.; Sarhan, A. *Makromol. Chem.* **1977**, *178*, 2799.
(14) Wulff, G.; Vietmeier, J. V.; Poll, H. G. *Makromol. Chem.* **1987**, *188*, 731.
(15) Wulff, G.; Poll, H. G. *Makromol. Chem.* **1987**, *188*, 741.
(16) Sellergren, B. *Am. Lab.* **1997**, *29*, 14.
(17) Katz, A.; Davis, M. E. *Macromolecules* **1999**, *32*, 4113.
(18) Duffy, D. J.; Das, K.; Hsu, S. L.; Penelle, J.; Rotello, V. M.; Stidham, H. D. *ACS Prepr. PMSE* **2000**, *82*, 69.
(19) Breinlinger, E.; Niemz, A.; Rotello, V. M. *J. Am. Chem. Soc.* **1995**, *117*, 5379.

10.1021/ja0201146 CCC: $22.00

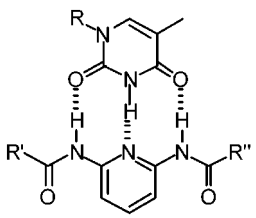

(1)

Figure 1. Three-point hydrogen-bonded recognition dyad based on thymine and 2,6-diacyldiaminopyridine used in this study.

monitor binding processes before and after polymerization, as well as rebinding with infrared spectroscopy.

This type of motif has been used previously; a very different polymer matrix is employed.[22−24] To characterize both pre- and post-polymerization binding events, thin films are used. Due to their consistent macroscopic shape and the variety of synthetic conditions that can be used during preparation (polymerization temperature, rate, light flux in the case of photoinitiated polymerizations), films provide the ideal platform for fundamental studies.[25−27] In addition, the film platform lends well to sensor applications and can be characterized with a variety of techniques allowing for a comprehensive characterization of the model system at different length scales. The polymeric matrix component, tripropylenegylcol diacrylate (TPGDA), is utilized in these studies, as its initiation and polymerization chemistry is well-understood.[25−31]

In this paper, we report the fabrication of thin films based on recognition element **1** and its characterization by infrared spectroscopy. The efficiency of the process and the reversibility of the films are quantified, providing insight into the mechanics of polymer imprinting.

Experimental Section

General. All chemicals were purchased from Aldrich and used as received. Solvents were purchased from VWR. CH_2Cl_2 was distilled over CaH_2. All reactions were carried out under Ar with oven-dried glassware. All synthesized compounds are stored in the dark and under refrigeration to avoid photodegredation or thermal degradation. All relevant infrared data are summarized in Table 1. NMR spectra were recorded on a Bruker 200 MHz spectrometer. Elemental analyses were performed by the Microanalytical Lab at the University of Massachusetts, Amherst.

***N*(3)-Dodecylthymine (2).** A solution of thymine (2.0 g, 15.8 mmol), dodecyl bromide (4.18 mL, 17.4 mmol), and K_2CO_3 (2.4 g, 17.4 mmol) were stirred in DMF (50 mL) at 45 °C for 2 days. Water (60 mL) was added to the yellow solution and the resulting mixture was extracted with ether (2 × 100 mL). The organic layers were collected and extracted with brine (2 × 100 mL). The organic layer was dried over $MgSO_4$ and dried by rotary evaporation and the residue purified by column chromatography (2:1 v/v hexanes−ethyl acetate). Yield 1.87 g, 40%. ^{1}H NMR ($CDCl_3$, 200 MHz) δ 0.88 (t, 3H, 14 Hz), 1.25 (m, 20 H), 1.93 (s, 3 H), 3.68 (t, 3 H, 15 Hz), 6.98 (s, 1H), 8.17 (b, 1H). Anal. Calcd for $C_{17}H_{30}N_3O_2$: C, 69.3; H, 10.27; N, 9.5. Found: C, 69.50; H, 10.41; N 9.57.

Table 1. Characteristic Vibrational Frequencies of NH and ND Stretching Vibrations

ν(NH) (cm^{-1})	ν(ND) (cm^{-1})	ν(NH)/ν(ND)
3419	2535	1.348
3270	2479	1.319
3210	2431	1.320
3165	2373	1.333

Diacryolyl-2,6-diaminopyridine (3). To a solution of 2,6-diaminopyridine (1.0 g, 9.2 mmol), triethylamine (2.83 mL, 20.0 mmol, 2.2 equiv), and CH_2Cl_2 (75 mL) was added acryloyl chloride (1.63 mL, 20.0 mmol) slowly over 15 min. The round-bottom flask was covered with aluminum foil and stirred overnight. Solvent was removed by rotary evaporation, and the resulting red solid was dissolved in ethyl acetate (100 mL) and successively extracted with brine (100 mL), saturated sodium bicarbonate (100 mL), and 0.1 M HCl (75 mL). The organic layer was collected and dried by $MgSO_4$, and the residue was purified by column chromatography (1:1 hexanes−ethyl acetate). The resulting white solid was vacuum dried overnight. Yield 1.68 g, 83%. ^{1}H NMR ($CDCl_3$, 200 MHz) δ 5.86 (d, 2 H, 14 Hz), 6.26 (q, 2 H, 18), 6.51 (d, 2H, 14 Hz), 7.30 (s,b 2 H), 7.78 (t, 1H, 11 Hz), 8.01 (d, 2 H, 15 Hz). Anal. Calcd for $C_{11}H_{11}N_3O_2$: C, 60.82; H, 5.10; N, 19.34. Found: C, 60.75; H, 5.11; N 19.45.

Film Preparation and Polymerization. Cross-linked polymer films were prepared by photoinitiated free-radical polymerization of tripropyleneglycol diacrylate (TPGDA) with Irgacure 369 (0.5 wt %) for photoinitiation. Monomer solutions were retained between cover glass slides (22 mm^2) on a temperature-controlled plate situated within a reaction vessel purged with nitrogen (5 min). Solutions were exposed to 50 mW·cm^{-2} of radiation from a Light-Welder 3010EC (DYMAX) for 10 s. A light guide delivered the radiation, a timed shutter regulated the exposure time, and a International Light IL390B Light Bug was used for intensity calibration. Films of controllable thickness have been prepared by using procedures defined previously.[25,28−30] The power spectrum of the source and the absorption characteristics of Irgacure 369 are well-matched, this is an important consideration in the selection of the proper photopolymerization conditions. Films of 100 μm thickness (measured with a micrometer) were used for infrared measurements. The sample temperature was monitored during film preparation by placing a thermocouple in contact with the glass slides. A glass capillary tube containing the polymerizable components was used to measure temperature rise in bulk polymerizations. The tubes were exposed to 10 mW/cm^2 of radiation for 180 s while the temperature was recorded electronically.

Characterization by Infrared Spectroscopy. A temperature-controlled infrared NaCl liquid cell of fixed thickness (0.1 mm) was used to measure solution-phase infrared spectra. The spectrum of the TPGDA monomer was obtained directly on a KBr plate. The minimum temperature that we can work with for the solution studies is 10 °C. This limitation does not exist for the film measurement. All infrared spectra were recorded at 2 cm^{-1} resolution with a Perkin-Elmer Spectrum 2000 FTIR equipped with both narrow and wide band MCT detectors. Titration experiments consisted of eight solutions with a constant host molecule concentration of ∼0.2 mol·L^{-1} in $CHCl_3$. The guest molecule concentration varied from 0 to 1.5 mol equiv over the set of eight solutions. An analogous set of titration solutions was prepared in TPGDA and pTPGDA, using ∼0.08 mol·L^{-1} host molecule.

(20) Nowick, J. S.; Feng, Q.; Tjivikua, T.; Rebek, J. *J Am Chem Soc* **1991**, *113*, 8831.
(21) Geib, S. J.; C., H. S.; Vicent, C.; Hamilton, A. D. *J. Chem. Soc., Chem. Commun.* **1991**, 1283.
(22) Tanabe, K.; Takeuchi, T.; Matsui, J.; Ikebukuro, K.; Yano, K.; Karube, I. *J. Chem. Soc., Chem. Commun.* **1995**, 2303.
(23) Yano, K.; Tanabe, K.; Takeuchi, T.; Matsui, J.; Ikebukuro, K.; Karube, I. *Anal. Chim. Acta* **1998**, *363*, 111.
(24) Kugimiya, A.; Mukawa, T.; Takeuchi, T. *Analyst* **2001**, *126*, 772.
(25) Stolov, A. A.; Xie, T.; Penelle, J.; Hsu, S. L. *Macromolecules* **2000**, *33*, 6970.
(26) Stolov, A. A.; Xie, T.; Penelle, J.; Hsu, S. L. *Macromolecules* **2001**, *34*, 2865.
(27) Stolov, A. A.; Xie, T.; Penelle, J.; Hsu, S. L.; Stidham, H. D. *Polym. Eng. Sci.* **2001**, *41*, 314.
(28) Decker, C. *J. Polym. Sci.: Part A: Polym. Chem.* **1992**, *30*, 913.
(29) Decker, C.; Decker, D.; Morel, F. In *Photopolymerization Fundamentals and Applications*; Scranton, A. B., Bowman, C. N., Peiffer, R. W., Eds.; American Chemical Society: Washington, DC, 1997; Vol. 673.
(30) Scherzer, T.; Decker, U. *Polymer* **2000**, *41*, 7681.
(31) Marx, S.; Liron, Z. *Chem. Mater.* **2001**, *13*, 3624.

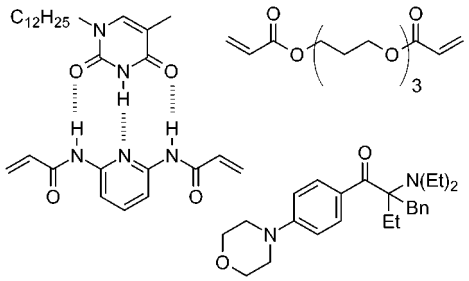

Figure 2. Chemical structures of host−guest complex, tripropyleneglycol diacrylate (TPGDA), and photoinitiator (Irgacure 369).

This concentration was used as it is the solubility limit of the host−guest complex in TPGDA. Deuterium-substituted host and guest molecules were prepared with D_2O and $CDCl_3$.

Transport Properties. Guest molecule extraction was accomplished by placing imprinted films in $CHCl_3$ for 6 h. After evaporation of the solvent, infrared spectra were recorded. Extracted films were placed in a 0.1 mol·L^{-1} solution of guest molecule in $CHCl_3$. Films were removed after 6 h and dried, and the spectrum was recorded. The films were subject to a second extraction experiment. The solutions used for extraction experiments were concentrated by evaporation and examined by infrared spectroscopy to confirm the release and uptake of the guest molecule. The rate of guest molecule release was measured by placing 1−2 mg of imprinted film in a 1 cm quartz cell containing $CHCl_3$. The absorbance spectrum of the solution was recorded between 190 and 800 nm with a Hewlett-Packard 8452A diode array spectrometer at 1 min intervals. The characteristic absorbance of *N*(3)-dodecylthymine at 274 nm is used to monitor its release from the imprinted films.

Results and Discussion

Characterization of the Host−Guest Complexes by Infrared Spectroscopy. Vibrational spectroscopy has been used extensively to study intra- and intermolecular hydrogen-bonding interactions[32−35] and was used in this study to characterize the host−guest complex **1**. The vibrational frequencies of OH and NH stretching vibrations typically shift to lower frequencies upon hydrogen bonding and the intensity of the shifted stretching vibrations is a direct measurement of complex concentration. These changes in the spectrum due to hydrogen bonding make infrared spectroscopy a powerful tool for examining intermolecular interactions. The infrared spectrum of the isolated host and guest molecules in chloroform and TPGDA are presented in Figure 3. Bands at 3419 and 3396 cm^{-1} are assigned to the free (non-hydrogen bonded) NH-stretching vibrations of the host and guest molecules in $CHCl_3$, respectively.[36−40] The lower frequency amide-(I,II) region is typically used for quantitative analysis because the higher frequency amide-A region can be complicated by carbonyl overtones, intense OH and CH stretching vibrations.[41] For our system, the amide-(I,II) vibrations of the of the host and guest molecules overlap with intense TPGDA bands, making the amide-A region the only window for characterization of the complex.

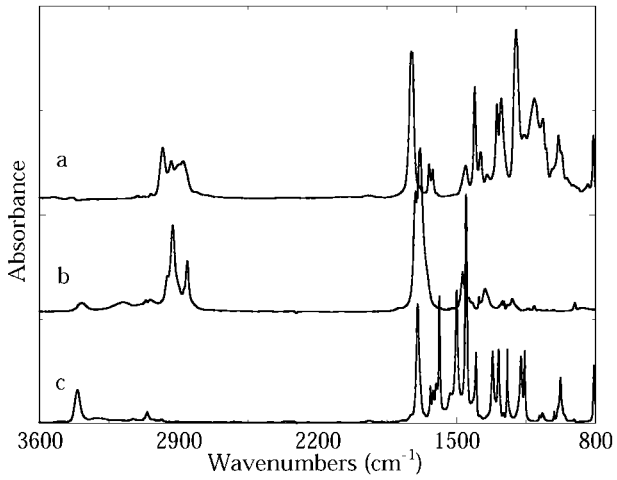

Figure 3. Infrared spectrum between 800 and 3600 cm^{-1} of (a) TPGDA, (b) guest, and (c) host molecules.

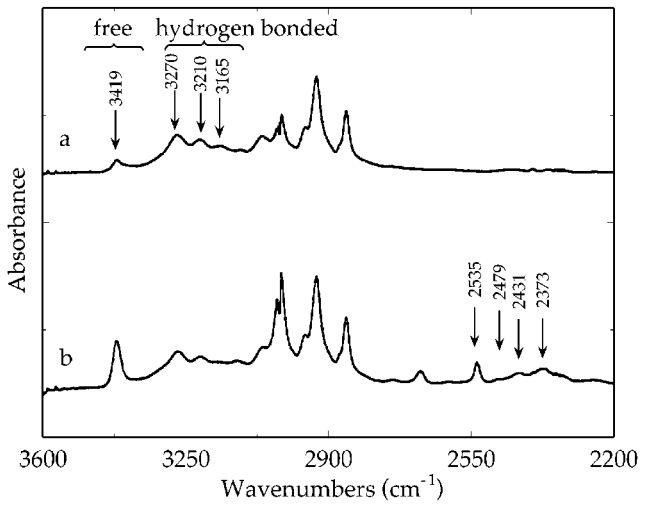

Figure 4. Infrared spectrum of chloroform solution (a) containing both host and guest molecules and (b) containing a mixture of the deuterium exchanged host and guest molecules. The frequencies of the NH and ND stretching vibrations have been annotated.

The infrared spectrum of solutions containing a mixture of host and guest molecules above 2000 cm^{-1} is shown in Figure 4a and deuterated analogues in Figure 4b. The three bands at 3165, 3210, and 3270 cm^{-1} are assigned to the hydrogen-bonded host−guest complex based on assignments for base pairs[38,40,42−44] and the isotopic substitution data. Isotopic substitution has been used to assign vibrations of complex molecules involved in hydrogen-bonding interactions.[41,45−47] Exchanging the hydrogen atoms in the amide groups (NH) with deuterium (ND) will shift the NH stretching vibrations to lower frequency. In the harmonic oscillator approximation, the ratio of the NH-to-ND frequencies is 1.359 with a 1% anharmonicity correction.[48] The observed frequency shifts are presented in Table 1 and are close to the

(32) Nakamoto, K.; Margoshes, M.; Rundle, R. E. *J. Am. Chem. Soc.* **1955**, *77*, 6480.
(33) Tsuboi, M. *J. Am. Chem. Soc.* **1959**, *81*, 1406.
(34) Jeffrey, G. A. *An Introduction to Hydrogen Bonding*; Oxford Universiy Press: New York, NY, and Oxford, UK, 1997; p 303.
(35) Noda, I.; Liu, Y.; Ozaki, Y. *J. Phys. Chem.* **1996**, *100*, 8665.
(36) Snyder, R. G.; Chen, L. X. Q.; Srivatsavoy, V. J. P.; Strauss, H. L.; Kubota, S. *J. Phys. Chem.* **1995**, *99*, 2214.
(37) Miyazawa, T. *J. Mol. Spectrosc.* **1960**, *4*, 168.
(38) Yanson, I. K.; Teplitsky, A. B.; Sukhodub, L. F. *Biopolymers* **1979**, *18*, 1149.
(39) Yang, J.; Gellman, S. H. *J. Am. Chem. Soc.* **1998**, *120*, 9090.
(40) Carmona, P.; Molina, M.; Lasagabaster, A. *J. Phys. Chem.* **1993**, *97*, 9519.
(41) Krimm, S.; Dwivedi, M. *J. Raman Spectrosc.* **1982**, *12*, 133.
(42) Buchet, R.; Sandorfy, C. *J. Phys. Chem.* **1984**, *88*, 3274.
(43) Buchet, R.; Sandorfy, C. *J. Phys. Chem.* **1983**, *87*, 275.
(44) Tsiourvas, D.; Sideratou, Z.; Haralabakopoulos, A. A.; Pistolis, G.; Paleos, C. M. *J. Chem. Phys.* **1996**, *100*, 14087.
(45) Miyazawa, T.; Shimanouchi, T.; Mizushima, S. I. *J. Chem. Phys.* **1956**, *24*, 408.
(46) Miyazawa, T.; Shimanouchi, T.; Mizushima, S. I. *J. Chem. Phys.* **1958**, *29*, 611.
(47) Rodriguez-Casado, A.; Carmona, P.; Molina, M. *J. Phys. Chem. B* **1998**, *102*, 5387.

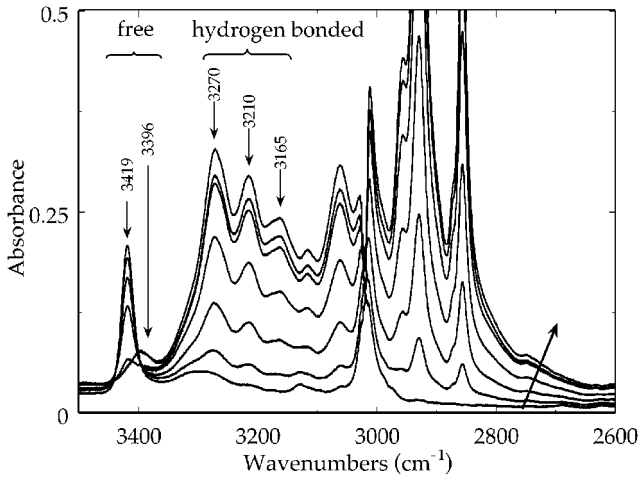

Figure 5. Infrared spectrum of titration solutions prepared in chloroform. The bold arrow denotes increasing guest molecule concentration and the frequencies of the free and hydrogen-bonded NH stretching vibrations have been annotated.

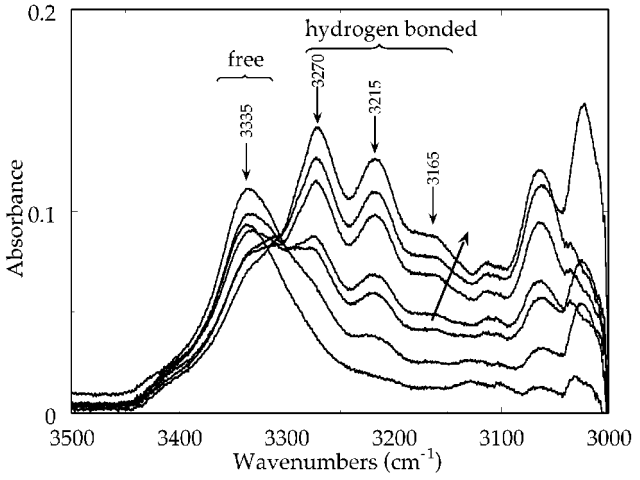

Figure 6. Infrared spectrum of titration solutions prepared in TPGDA. The bold arrow denotes increasing guest molecule concentration and the frequencies of the free and hydrogen-bonded NH stretching vibrations have been annotated.

predicted values, supporting the assignments made for host−guest complex bands in the amide-A region.

The appearance of three distinct hydrogen-bonded NH vibrations is notable. Examining the structure of the complex (Figure 2), at least two stretches due to hydrogen bonds are expected as the two (NH···O) bonds are expected to be different in energy from the (NH···N) bond.[32,34,49] It is the appearance of the third hydrogen bond NH stretching vibration that is significant. This indicates that the two (NH···O) bonds are energetically distinct. The NH stretching vibrations are sensitive to both the depth and shape of the potential energy surface describing their vibration.[34] The two energetically distinct (NH···O) bonds may result from the C_{12} alkyl group on the guest molecule. The presence of the alkyl tail may affect the bond lengths and angles of the complex through steric influence.[50] The vibrational spectrum of the hydrogen-bonded complex is sensitive to the structure of the complex.[32,34,51]

Determination of the Binding Constant (*K*) Before and After Polymerization. The infrared spectra of the complex in chloroform and TPGDA are shown in Figures 5 and 6, respectively. The presence of the 3270, 3215, and 3165 cm^{-1} bands in the TPGDA monomer solutions (Figure 6) definitively establishes the presence of the host−guest complex before cross-linking of TPDGA occurs. The free NH stretch of the host molecule at 3419 cm^{-1} in chloroform (Figure 5) shifts to 3340 cm^{-1} in TPGDA (Figure 6) due to interactions between the host molecule and TPGDA.

A relationship between the intensities of the NH vibrations and the binding constant is presented to allow interpretation of the experimental data and quantify the association (binding constant). Equation 1 represents the (1:1) binding reaction between the host (H) and guest (G) molecules to form the hydrogen-bonded complex (HG). The formation of a (1:1) complex between the host molecule and thymine or flavin derivatives via multiple hydrogen bonds has previously been established.[52] The standard equilibrium constant (K) for this reaction is given by (1) where [H] and [G] are the concentrations of the free host and guest molecules and [HG] is the concentration of the host−guest complex. Equation 1 can be rearranged in order to use the free host and guest molecule concentrations and the experimental absorbance values of the complex to determine K. The free host molecule concentration [H] is written in terms of its initial concentration [H°] and the complex concentration [HG]. Substitution into eq 1 and rearranging yields eq 2, which expresses the complex concentration [HG] in terms of K, [G], and [H°]. This and several other useful binding isotherms have been reported previously.[53] [HG] in eq 2 is written in terms of its absorbance (A_{cplx}) and rearranged to obtain eq 3. The coefficient (α) is a product of several quantities given by eq 4, where (ϵ_{cplx}) is the absorption coefficient of the complex. The values of K and α are determined from a nonlinear least-squares fit of eq 3 to the absorption, free guest molecule concentration data. This approach does not require prior knowledge of the absorption coefficient of the complex or approximations about its value to be made. Binding constants determined at different temperatures allow the change in free energy ($\Delta G(T)$), enthalpy (ΔH), and entropy (ΔS) of the binding

$$K = \frac{[HG]}{[H]\cdot[G]} \tag{1}$$

$$[HG] = \frac{[H^\circ]\cdot[G]\cdot K}{1 + K\cdot[G]} \tag{2}$$

$$A_{cplx} = \frac{\alpha\cdot[G]}{1 + K\cdot[G]} \tag{3}$$

$$\alpha = [H^\circ]\cdot\epsilon_{cplx}\cdot K \tag{4}$$

(48) Wilson, J. E. B.; Decius, J. C.; Cross, P. C. *Molecular Vibrations. The theory of infrared and Raman vibrational spectra*; McGraw-Hill Book Company, Inc.: New York, 1955; p 388.
(49) Joesten, M. D.; Schaad, L. J. *Hydrogen Bonding*; Marcel Dekker: New York, 1974; p 622.
(50) Wallqvist, A.; Covell, D. G. *J. Phys. Chem.* **1995**, *99*, 13118.
(51) Pimentel, G. C.; Sederholm, C. H. *J. Chem. Phys.* **1956**, *24*, 639.
(52) Greaves, M. D.; Rotello, V. M. *J. Am. Chem. Soc.* **1997**, *119*, 10569.
(53) Klotz, I. M. *Ligand−Receptor Energetics: A guide for the perplexed*; John Wiley & Sons: New York, 1997; p 170.

Table 2. Thermodynamic Parameters Determined for the Host−Guest Complex

temp, °C	K (M^{-1})
TPGDA solutions[a]	
10	900(±122)
20	249(±50)
35	204(±39)
TPGDA films[a]	
5	39(±10)
20	27(±7)
35	23(±6)

	ΔH (kJ mol^{-1})	ΔS (kJ mol^{-1} K^{-1})
solutions	−55(±12)	−0.14(±0.03)
films	−12(±8)	−0.013(±0.008)

[a] Host molecule concentration, 0.08 M.

to be obtained from standard thermodynamic relationships.[54] The error in the fitted parameters was estimated by statistical methods.[55]

The values of [H] and [G] in the chloroform solutions were calculated from the intensities of the NH-stretching vibrations at 3419 and 3396 cm^{-1}. The concentration of the free host molecule in TPGDA solutions was calculated from the intensity of the 3335 cm^{-1} band, the free host NH stretch in TPGDA. The concentration of the bound guest molecule is calculated from the free host molecule concentration with use of the (1:1) binding stoichiometry.[52] The peak height was used as the intensity in all concentration and binding constant calculations.

The binding constant describing the equilibrium between the free and bound states can be used to compare the state of the complex in different media. The thermodynamic binding constants collected in Table 2 were calculated in TPGDA, $CHCl_3$, and CH_2Cl_2 and are 148(±40), 236(± 53), and 417(±100) M^{-1}, respectively. These values correspond to 0.88, 0.91, and 0.96 mol % of complex present. As the polarity of the solvent increases (CH_2Cl_2 to $CHCl_3$ to TPGDA), the binding constant decreases. It is also known that weak hydrogen-bonding interactions with $CHCl_3$ exist, competing for Lewis basic sites. Interactions between the carbonyl groups of TPGDA and the NH groups of free host and guest molecules are present and evidenced by the band at 3340 cm^{-1}. The competitive interactions do not, however, significantly diminish the prepolymerization binding constant.

Determination of the enthalpy of association before and after cross-linking is performed to describe the molecular imprinting efficiency in a quantitative fashion. These values also provide a comparison to other systems with multiple hydrogen bonds and validate our infrared analysis. Binding isotherms obtained in TPGDA are shown in Figure 7. The values of K, ΔH, and ΔS obtained from the isotherms are given in Table 2. The analysis based on the infrared spectra in the amide-A region produces binding enthalpies similar to those of other complexes involving multiple hydrogen bonds. The binding enthalpy in TPGDA of 55 kJ·mol^{-1} (13 kcal·mol^{-1}) is comparable to the values reported for adenine-uracil (AU),[38] adenine-thymine (AT),[38] and cytidine-guanosine (CG)[40] base pairs, with values of 14.5, 13.0 , and 13.6 kcal·mol^{-1}, respectively.

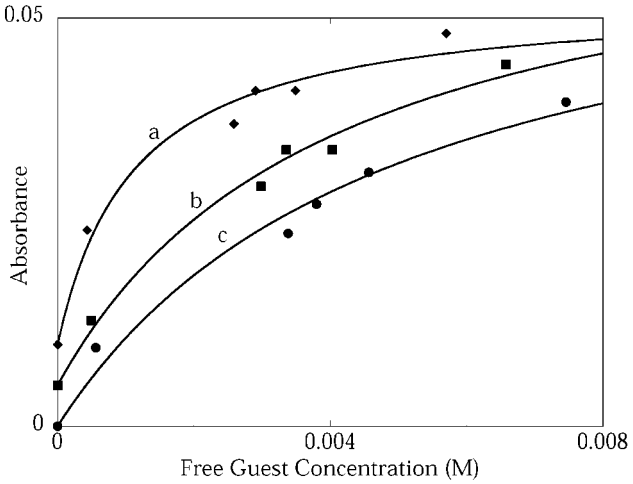

Figure 7. Binding isotherms obtained in TPGDA solutions at (a) 10, (b) 20, and (c) 35 °C. Isotherms a and b have been shifted vertically for plotting purposes.

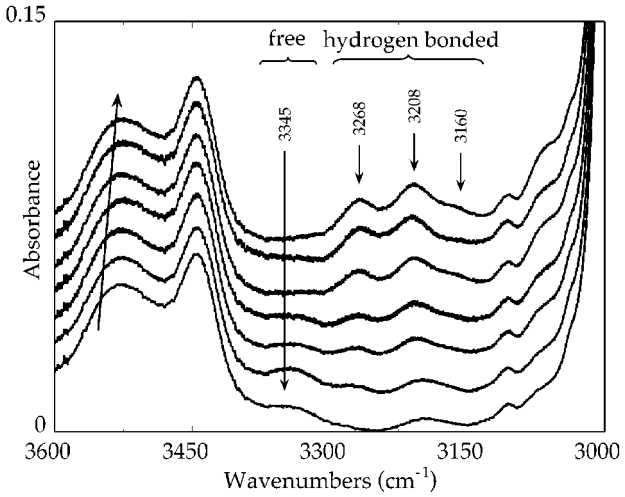

Figure 8. Infrared spectrum of imprinted TPGDA films prepared from the titration solutions. The bold arrow indicates the direction of increasing guest molecule concentration. The frequencies of the free and hydrogen-bonded NH stretching vibrations have been annotated.

Figure 8 shows the infrared spectrum of cross-linked films prepared from TPGDA titration solutions. The presence of three hydrogen-bonded NH vibration bands indicates that the host−guest complex is present in the films. Stability of the post-polymerization complex is indicated by the observations that the frequencies of the NH stretching vibrations (3268, 3208, and 3160 cm^{-1}) are not significantly shifted from the prepolymerization values (3270, 3213, and 3161 cm^{-1}). Absorption data in the amide-A region are treated the same way as the solution-phase data to obtain an apparent binding constant in the polymer films. It should be noted that the binding constant calculated for the cross-linked films is not necessarily the thermodynamic binding constant, as the populations measured may represent kinetically trapped states. Binding isotherms for films prepared at different temperatures are presented in Figure 9 and binding constants summarized in Table 2. Binding constants in the cross-linked films are on average a factor of 10 smaller compared to the state before cross-linking. This can be attributed to a change in the binding enthalpy or entropy (thermodynamic changes) associated with reduction in segmental dynamics due to cross-linking.

(54) Berry, R. S.; Rice, S. A.; Ross, J. *Physical Chemistry*, 2nd ed.; Oxford University Press: New York, NY, and Oxford, UK, 2000; p 1064.
(55) Shoemaker, D. P.; Garland, C. W.; Nibler, J. W. *Experiments in Physical Chemistry*, 6th ed.; McGraw-Hill Companies, Inc.: New York, 1996.

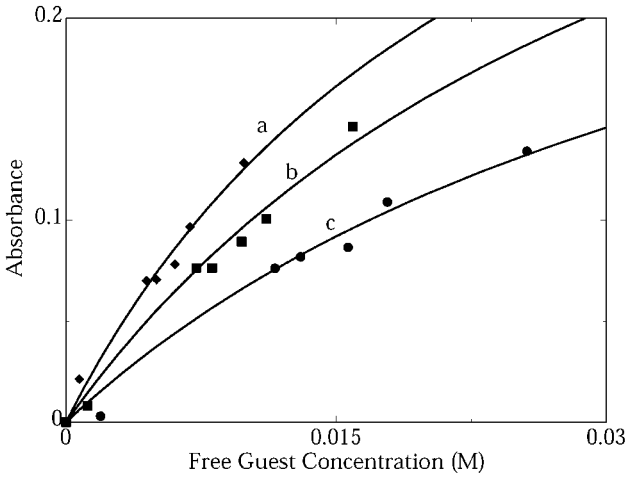

Figure 9. Binding isotherms obtained from TPGDA films polymerized at (a) 5, (b) 20, and (c) 35 °C.

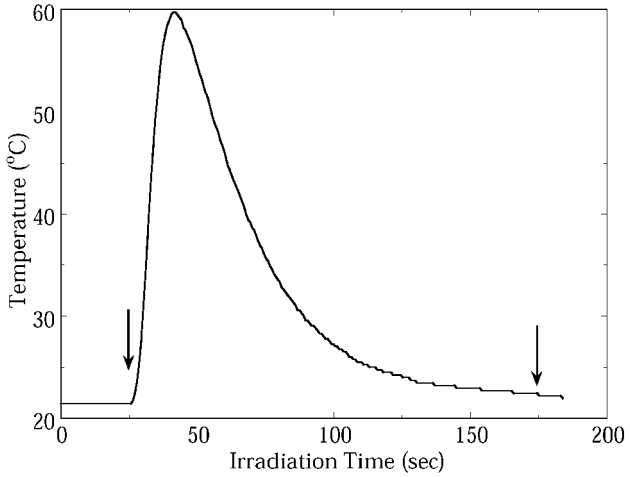

Figure 10. Measured temperature increase during polymerization of TPGDA. The arrows indicate the beginning and end of exposure of the sample to radiation.

The energy released during the polymerization of acrylates is known to be significant and the local temperature may rise substantially during the polymerization if heat is not properly dissipated.[25,56] A reduction in chain dynamics can also be induced by this temperature variation. Figure 10 shows the measured temperature profile for a bulk polymerization of TPGDA, in which the maximum temperature change observed was 38 °C. The maximum temperature change observed during polymerization of the imprinted films was 5 °C, suggesting that thermal effects do not significantly contribute to the value of the binding constant. As well, polymerizing at lower temperatures only produced a slight increase in the binding constants (Table 2), indicating that the decrease in the observed binding constant can be attributed to an increase in molecular confinement after polymerization, resulting in changes in the local environment of the binding cavity.

The shift in frequency of a free NH and a bound NH in the infrared spectrum can be used as a measure of the strength and nature of a hydrogen-bonding interaction. The width of the vibrational band represents the distribution of hydrogen-bonding states. The hydrogen-bonded NH vibrations in the cross-linked

(56) Flory, P. J. *Principles of Polymer Chemistry*; Cornell University Press: Ithica, NY, 1953.

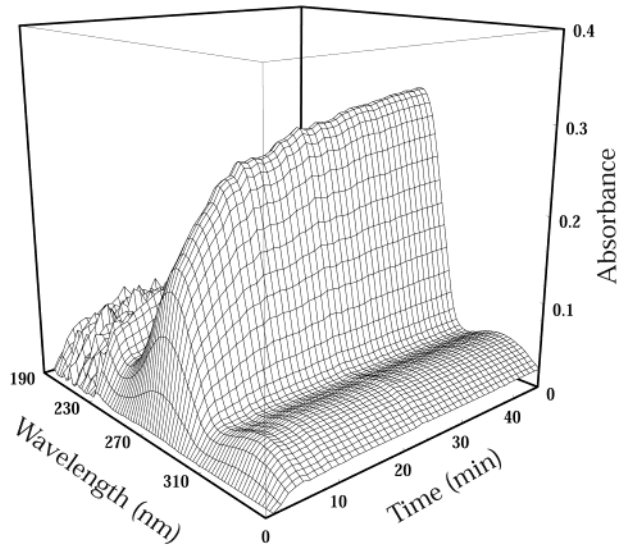

Figure 11. Release of guest molecule from imprinted film monitored by UV−visible spectroscopy. Absorbance maximum at 274 nm is characteristic of the guest molecule.

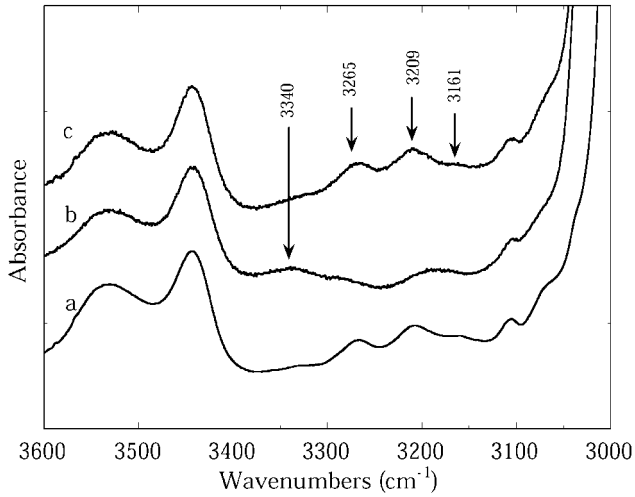

Figure 12. Infrared spectrum of imprinted TPGDA films (a) pre-extraction, (b) post-extraction, and (c) post-uptake. Frequencies of the free and hydrogen-bonded NH stretching vibrations have been annotated.

films are not shifted from the frequencies in the monomer, indicating that the hydrogen-bonding interactions in the cross-linked films have the same strength (ΔH). However, the width and intensity of the bands in the films is different from that of the monomer. This indicates that the number of hydrogen-bonding states in the films is different from that of solutions resulting from a change in the local environment. During cross-linking the host, guest, and reacting monomer molecules lose translational and rotational degrees of freedom. This loss in entropy does not preclude films with high binding affinity from being prepared. On the basis of spectroscopic data, the binding enthalpy was calculated to be $-12(\pm 8)$ kJ·mol^{-1} in the cross-linked films and $-55(\pm 12)$ kJ·mol^{-1} in the monomer.

The decrease in the observed energy of the binding interactions before and after polymerization can be attributed to shrinkage during cross-linking, rather than a change in the strength of the three-point interaction after polymerization. Stolov et al. reported the onset of stress development during the cure of TPGDA to be coincident with the gel point.[25] If the

mechanical stress cannot be efficiently relieved, this may result in the constriction or confinement of the pore structure in the matrix, which could result in mechanical deformation of the host−guest complex in the films resulting in width or intensity changes of the NH stretching vibrations.

Transport Properties. The guest molecule has a characteristic absorption maximum at 274 nm. This allows its release from the imprinted films into solution to be monitored by UV−visible spectroscopy. Figure 11 presents the UV−visible spectrum of the $CHCl_3$ extraction solution as a function of time. The spectrum demonstrates that under relatively mild extraction conditions the template molecule can be removed in a reasonable amount of time. Timely transport is an important attribute for imprinted materials for use in thin film sensing applications.

The transport of the guest molecule should also be observable in the infrared spectra of the extracted films. The infrared spectra of the films before extraction, after extraction, and after the uptake experiments are shown in Figure 12, panels a, b, and c, respectively, and demonstrate reversibility in our imprinted film. The spectra of the extracted films (Figure 12b) all lacked the 3270 cm^{-1} band of the complex while the 3335 cm^{-1} band characteristic of the host molecule in the matrix was observed. The 3270 cm^{-1} band reappeared in the infrared spectrum of the uptake films (Figure 12c), indicating that guest molecules diffused back into the film and bound to the host molecule sites. This presents direct spectroscopic evidence that both molecular transport and binding occur in these imprinting films. The TPGDA matrix allows transport of the guest molecule and retains the recognition ability imparted to it by covalent incorporation of the host molecule.

Conclusions

We have designed a model system to characterize molecular imprinting. Three-point hydrogen bonding and thin films were characterized by infrared spectroscopy. This model system provides a scaffold to study changes in the host−guest hydrogen-bonding interactions and changes in the structure of the TPGDA matrix simultaneously. This study presents a method for quantitatively measuring and comparing the degree of interaction between recognition elements in imprinted polymer systems. A 10-fold difference between the pre-polymerization binding constant and the apparent binding constant after polymerization in the films has been observed. The possible contribution of sample heating during polymerization on the apparent binding constants was considered. We conclude that change in the local environment of the binding pocket is the primary contributor to the state of the molecular interaction post-polymerization.

The transport and binding properties of an imprinted material determine its utility. Desired applications of imprinted materials include real-time, rapid, or in vitro sensing applications. Removal of the imprint molecules from the films and reincorporating into the films has been directly demonstrated, indicating the feasibility of our approach for the design of imprinted material. This paper focuses on molecular aspects, while future contributions will analyze specific features at larger length scales.

Acknowledgment. This work was supported by the NSF-funded University of Massachusetts Materials Research Science & Engineering Center (DMR-9809365) and CHE-9905492.

JA0201146